Biochemical and Biophysical Research Communications 667 (2023) 104–110

Contents lists available at ScienceDirect

Biochemical and Biophysical Research Communications

journal homepage: www.elsevier.com/locate/ybbrc

Negative pressure induces dedifferentiation of hepatocytes via RhoA/ROCK pathway

Mahmoud Osman Khalifa [a, b, c], Takahito Moriwaki [a], Shouhua Zhang [d], Wei Zhou [e], Kosei Ito [c], Tao-Sheng Li [a, *]

[a] Department of Stem Cell Biology, Nagasaki University Graduate School of Biomedical Sciences, 1-12-4 Sakamoto, Nagasaki, 852-8523, Japan
[b] Department of Anatomy and Embryology, Veterinary Medicine, Aswan University, Aswan, Egypt
[c] Department of Molecular Bone Biology, Graduate School of Biomedical Sciences, Nagasaki University, 1-7-1 Sakamoto, Nagasaki, 852-8588, Japan
[d] Department of General Surgery, Jiangxi Provincial Children's Hospital, Nanchang, Jiangxi, China
[e] Department of Gastrointestinal Surgery, Jiangxi Provincial Cancer Hospital Nanchang, Jiangxi Province, China

ARTICLE INFO

Article history:
Received 21 April 2023
Received in revised form
8 May 2023
Accepted 13 May 2023
Available online 14 May 2023

Keywords:
Hepatocytes
Dedifferentiation
Stemness
RhoA/ROCK
Negative pressure

ABSTRACT

Biomechanical forces are known to regulate the biological behaviors of cells. Although negative pressure has been used for wound healing, it is still unknown about its role in regulating cell plasticity. We investigated whether negative pressure could induce the dedifferentiation of hepatocytes. Using a commercial device, we found that the exposure of primary human hepatocytes to −50 mmHg quickly induced the formation of stress fibers and obviously changed cell morphology in 72 h. Moreover, the exposure of hepatocytes to −50 mmHg significantly upregulated RhoA, ROCK1, and ROCK2 in 1–6 h, and dramatically enhanced the expression of marker molecules on "stemness", such as OCT4, SOX2, KLF4, MYC, NANOG, and CD133 in 6–72 h. However, all these changes in hepatocytes induced by −50 mmHg stimulation were almost abrogated by ROCK inhibitor Y27623. Our data suggest that an appropriate force of negative pressure stimulation can effectively induce the dedifferentiation of hepatocytes via RhoA/ROCK pathway activation.

1. Introduction

Dedifferentiation is well known to be a transient process in which specialized cells turn back to an earlier stage of differentiation characterizing by less identical function and phenotype. Although there has almost an era history about the concept of dedifferentiation, it becomes one of the hottest topics on cell biology since the success of inducing mouse and human fibroblasts into embryonic stem-like pluripotent stem cells by the transduction of Yamanaka four factors OCT4 (Octamer-binding transcription factor 4), SOX2 (Sex determining region Y-box 2), KLF4 (Kruppel like factor 4), MYC (MYC proto-oncogene), NANOG (Nanog homeobox), and CD133 (prominin 1) [1,2]. However, there are safety problems and other disadvantages to the genetic transduction of exogenous factors into cells for future clinical application [3]. To lessen the genome intervention of host cells, other alternative methods/approaches, such as chemical compounds, RNAs, and miRNAs have been successfully used for cell reprogramming [4–6].

The hepatocytes are highly differentiated cells that carry out most of the hepatic functions. Although mature hepatocytes are generally known to have a short life span and very limited proliferative ability *in vitro*, vigorous regeneration of healthy liver following partial hepatectomy happens to restore the resected/defected part within a few weeks [7,8]. Similarly, the thoracic cavity following pneumonectomy may create a distension force to lead the shift of type II pneumocytes into type I pneumocytes for compensatory regeneration of lungs [9,10]. In contrast to the healthy liver, diseased livers are hardly regenerated because an inappropriate microenvironment, including the alteration of extracellular matrix stiffness is known to play a critical role in regulating the proliferation of hepatocytes and the differentiation of hepatic progenitors. Therefore, biomechanical forces are likely involved in the compensatory regeneration of the liver and lungs.

Biomechanical forces have been commonly recognized to play pivotal roles in physiological and pathological processes through various mechanotransduction signaling pathways. Basically, mechanotransduction can be elicited via cell-cell and cell-matrix

* Corresponding author.
E-mail address: litaoshe@nagasaki-u.ac.jp (T.-S. Li).

https://doi.org/10.1016/j.bbrc.2023.05.042
0006-291X/

interactions. Consequently, the pioneer regulatory pathway of mechanotransduction is based on RhoA/ROCK signaling, which initiates various downstream cascades. RhoA (Ras Homolog Family Member A) not only regulates cytoskeleton organization but also initiates or shares various pathways for cell proliferation and differentiation [11,12]. RhoA kinases Rho associated coiled-coil containing protein kinase 1 & 2 (ROCKs) are widely distributed in various tissue cells, where they have diverse roles in physiological and pathological processes [13,14]. Interestingly, it has recently been reported that inducing physical compression force to adipocytes by culturing in a hypertonic medium promotes the dedifferentiation of adipocytes through Wnt/β-catenin signaling [15]. Moreover, the dedifferentiated adipocytes have shown the abilities of long-term self-renewal and serial clonogenicity, but do not form teratomas [15]. Therefore, mechanical stress may be used as a simple and safe method for cell reprogramming. However, it is still poorly understood the precise role and mechanism of mechanical stress, especially the negative pressure in regulating cell differentiation/dedifferentiation.

In this study, we tested the hypothesis that an appropriate force of negative pressure stimulation may effectively induce cell dedifferentiation. By exposing human primary hepatocytes to −50 mmHg, we found that the RhoA/ROCK pathway was quickly activated, and then followed by an extensive upregulation of marker molecules on “stemness”, suggesting the dedifferentiation of hepatocytes.

2. Materials and methods

2.1. Cell culture

Human primary hepatocytes were purchased from the Sciencell Company (Catalog #5200). The cryopreserved hepatocytes were thawed rapidly in a 37 °C water bath. Cells were resuspended in the recommended hepatocytes medium (Sciencell, Catalog #5201) with the addition of 1% penicillin-streptomycin and 5% fetal bovine serum, and then cultured under 37 °C in a 5% CO_2 incubator. Cells were used for the following experiments.

2.2. Negative pressure stimulation

Negative pressure was induced to hepatocytes using a commercial device connected to a vacuum aspirator. Briefly, the hepatocytes were seeded in culture plates or dishes at the density of $1x10^5$ cells/cm^2, and left for attachment for 16 h. We further incubated the cells to achieve 60–80% confluence, and changed the medium without serum supplement [16]. Thereafter, cells were placed in a transparent acrylic negative vacuum chamber with a standard gauge that was set at −50 mmHg inside the incubator; without (NP group) or with the addition of 10 μM pan ROCK inhibitor Y27632 (ATCC® ACS-3030™) in medium (NP + Y27 group). As a control, cells were kept in the same incubator under atmospheric pressure (AP group).

2.3. Cell number and viability

The number and viability of hepatocytes were evaluated after treatments. Briefly, the hepatocytes were harvested, stained with 0.4% trypan blue (BIO-RAD, Cat.1450013), and counted by TC20 automated cells counter (BIO-RAD).

2.4. Immunofluorescence staining

Hepatocytes were seeded on clean glass coverslips incubated and treated as described above. Cells were fixed with 4% paraformaldehyde in PBS and permeabilized with 0.3% Triton X-100 (Sigma-Aldrich) in PBS solution for 20 min. After blocking with 5% bovine serum albumin in PBS, the cells were incubated with different primary antibodies (Supplementary Table 1) overnight at 4 °C and then incubated with the proper secondary antibodies (Supplementary Table 2) for 1 h in a dark humid chamber at room temperature. Then, the glass coverslips were mounted with VECTASHIELD Hardset Antifade mounting medium either with DAPI (4′,6-diamidino-2-phenylindole) (H-1500, Funakoshi) or TRITC-labeled phalloidin (H-1600, Funakoshi). The images were taken with a confocal fluorescent microscope (Olympus FV10i). For each staining, 10 images were taken from randomly selected fields, and the fluorescence intensity of staining was measured by Image J software.

2.5. RNA extraction and qRT-PCR

Total RNA was purified from hepatocytes using TRIzol reagents (ZYMO RESEARCH, USA), and then the concentration and purity were measured with NanoDrop™ 2000 spectrophotometer. The cDNA templates were reversely transcripted with SuperScript™ VILO™ reverse transcriptase reagent. The primers were synthesized and purchased from Hokkaido System Science CO., Ltd, Japan (Supplementary Table 3). The qPCR was done by THUNDERBIRD SYBR (Toyobo, Japan). All reactions were performed using the CFX96TM Real-Time PCR machine (BIO-RAD, USA). Relative expression levels of genes were normalized against *GAPDH*.

2.6. Statistical analysis

All data are presented as the mean ± SD (n = 3 in each group). Statistical analysis was performed either with one- or two-way analysis of variance and Tukey's multiple comparisons using GraphPad Prism software (version 8, Prism Academy, San Diego, USA). The significant differences between groups were considered at a minimum value of $p < 0.05$.

3. Results

3.1. Exposure of hepatocytes to −50 mmHg changes obviously cell morphology and slightly decreases cell viability

The cell morphology was observed under phase contrast microscopy at 1, 6, and 72 h of treatments. Under −50 mmHg stimulation, some hepatocytes showed a spherical morphology with condensed cytoplasm (Fig. 1A). In contrast, the hepatocytes treated with −50 mmHg and ROCK inhibitor Y27632 showed a fibroblast- or mesenchymal cell-like morphology (Fig. 1A). Compared with the AP group, the cell number and viability were significantly decreased at 6 or 72 h in both NP and NP + Y27 groups (Fig. 1B and C).

TRITC-Phalloidin staining of F-actin indicated that the cytoskeleton was detected as well-organized stress fibers in hepatocytes under −50 mmHg stimulation at 1, 6, and 72 h, suggesting the polymerization of actin filaments (Fig. 1D). However, the actin filament polymerization of hepatocytes under −50 mmHg stimulation was completely disturbed with the addition of ROCK inhibitor Y27632 in the medium (Fig. 1D).

Quantitative analysis on the area of cell nuclei and cytoplasm also showed that the ratio of nuclear area to the cytoplasmic area was significantly higher in the NP group in comparison to AP and NP + Y27 groups (Fig. 1E). At 72 h of the exposure to −50 mmHg, some hepatocytes were positively expressed with CK19, a marker of hepatic progenitor (Fig. 1F). Considering the morphological feature of the larger nucleus of hepatic progenitor [5], −50 mmHg

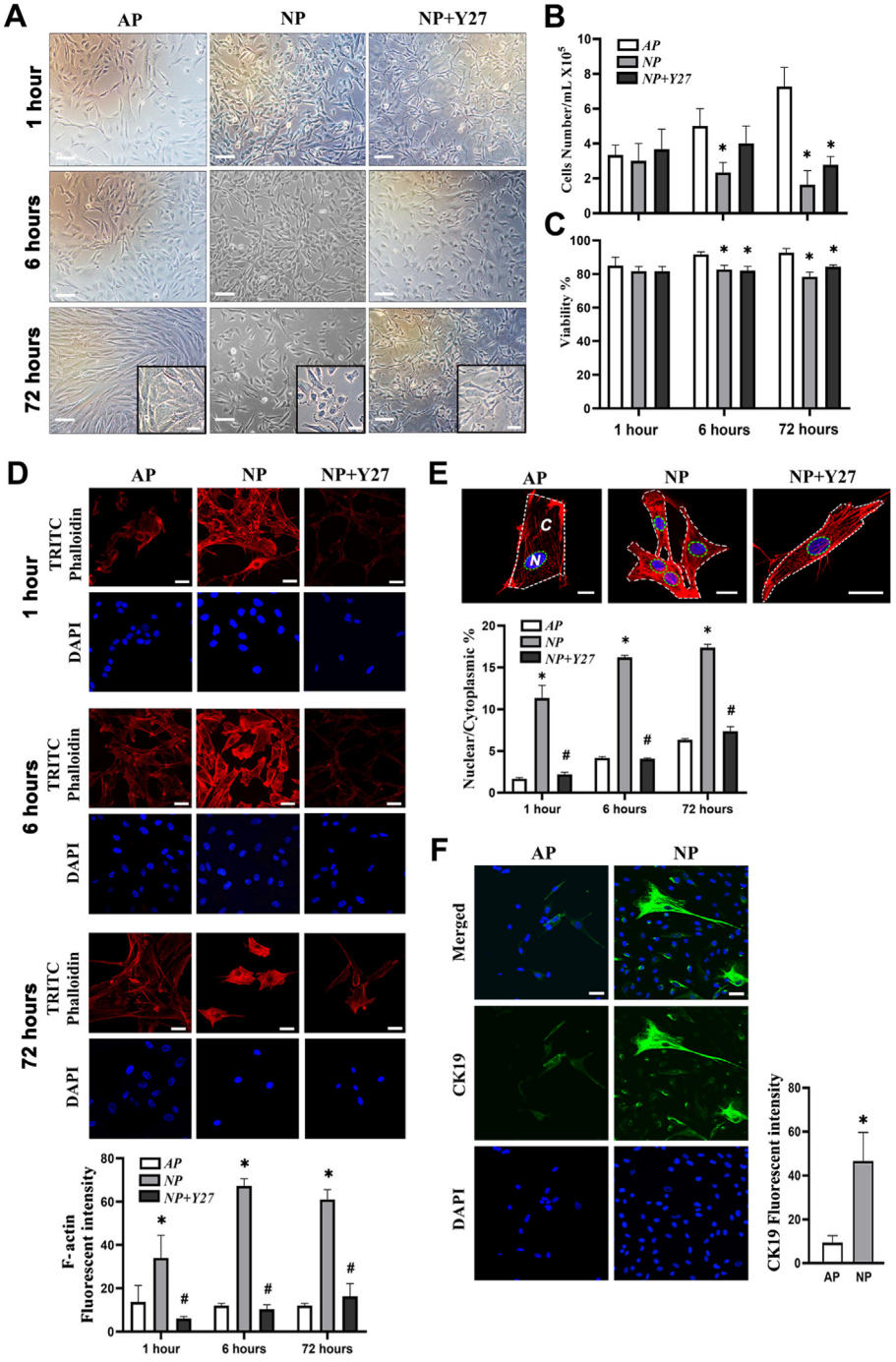

Fig. 1. The morphology, viability, and TRITC phalloidin staining of hepatocytes with −50 mmHg stimulation and ROCK inhibitor treatment. (**A**) Representative phase-contrast images show the morphology of hepatocytes (scale bars: 200 μm and 50 μm in insets). (**B & C**) Quantitative data on cells number and viability evaluating by trypan blue staining. (**D**) Representative images of TRITC phalloidin staining for F-actin stress fibers are shown (scale bars: 50 μm). The lower graph presents the quantitative data by measuring the fluorescence intensity. (**E**) Representative images and quantitative data of the nuclear to cytoplasm ratio are shown (scale bars: 100 μm). (**F**) Representative images and quantitative data of the immunofluorescence staining on CK19 are shown (scale bars: 50 μm). All data are presented as mean ± SD from three independent experiments. AP: atmospheric pressure; NP: negative pressure; NP + Y27: negative pressure plus ROCK inhibitor Y27632. *$p < 0.0001$ *vs.* AP group; #$p < 0.0001$ *vs.* NP group in all time points. (For interpretation of the references to colour in this figure legend, the reader is referred to the Web version of this article.)

stimulation for 72 h may be able to induce the dedifferentiation of some hepatocytes into hepatic progenitors.

3.2. Negative pressure induces the dedifferentiation of hepatocytes through RhoA/ROCK pathway

As one of the major mechanotransduction signaling pathways, the activation of the RhoA/ROCK pathway initiates the transcription of a variety of target downstream genes [17]. Our qRT-PCR data (Fig. 2A) and immunofluorescence staining analysis (Fig. 2B–D), consistently showed robust upregulation of RhoA, ROCK1, and ROCK2 in the NP group in 1–6 h ($p < 0.0001$ *vs.* AP group), suggesting the quick activation of RhoA/ROCK pathway in hepatocytes under −50 mmHg stimulation. Followed by the activation of the

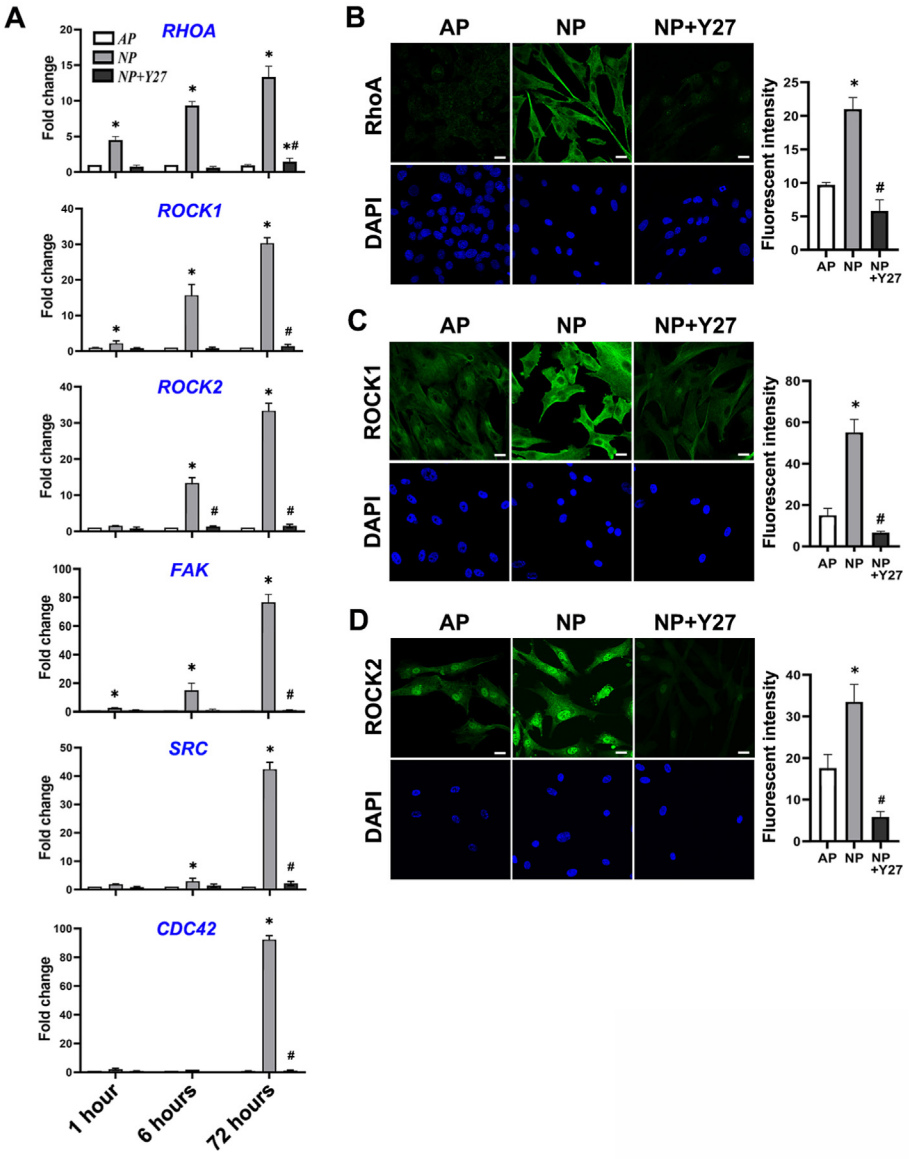

Fig. 2. The expression changes of molecules related to RhoA/ROCK signaling pathway in hepatocytes with −50 mmHg stimulation and ROCK inhibitor treatment. (**A**) qRT-PCR data on the expression of *RHOA*, *ROCK1*, *ROCK2*, *FAK*, *SRC*, and *CDC42* are shown. (**B-D**) Representative images (left) and semi-quantitative data (right bar graphs) show the immunofluorescence staining of RhoA (**B**), ROCK1 (**C**), and ROCK2 (**D**) at 72 h after treatment (scale bars: 100 μm). All data are presented as mean ± SD from three independent experiments. AP: atmospheric pressure; NP: negative pressure; NP + Y27: negative pressure plus ROCK inhibitor Y27632. $^{*}p < 0.0001$ *vs.* AP group; $^{\#}p < 0.0001$ *vs.* NP group in all time points.

RhoA/ROCK pathway, several downstream genes such as *FAK*, *SRC*, and *CDC42* were also significantly induced in hepatocytes, mostly at 6–72 h of stimulation with −50 mmHg ($p < 0.0001$ *vs.* AP group, Fig. 2A). Naturally, ROCK inhibitor Y27632 effectively blocked the activation of RhoA/ROCK pathway and attenuated the upregulation of downstream target genes in hepatocytes induced by −50 mmHg stimulation ($p < 0.0001$ *vs.* NP group, Fig. 2).

To confirm the role of negative pressure in inducing hepatocyte dedifferentiation, we further measured the expression of several marker molecules on "stemness", including CD133, OCT4, SOX2, MYC, KLF4, and NANOG in hepatocytes at different time points after treatments. qRT-PCR clearly showed that these marker molecules on "stemness" almost upregulated in hepatocytes at 6 h, and the expression of CD133 was also upregulated at 72 h under −50 mmHg stimulation (Fig. 3). Immunofluorescence staining also confirmed the enhancement of MYC, NANOG, and KLF4 in hepatocytes at protein level at 72 h under −50 mmHg stimulation (Fig. 4A–C). The ROCK inhibitor Y27632 effectively attenuated the enhancement on the expression of CD133, SOX2, NANOG, KLF4, and OCT4 in hepatocytes induced by −50 mmHg stimulation, although the enhanced expression of MYC was only partially attenuated (Figs. 3 and 4). These data suggest that −50 mmHg stimulation promotes the dedifferentiation and stemness acquisition of hepatocytes through the activation of the RhoA/ROCK pathway.

4. Discussion

Negative pressure is one of the mechanical forces used clinically for open wounds and fracture healing. It is based on suboptimal atmospheric pressure by applying a vacuum pumping machine. In this study, we investigated the possibility of negative pressure in inducing cell dedifferentiation. We found that hepatocytes with −50 mmHg stimulation robustly upregulated a series of

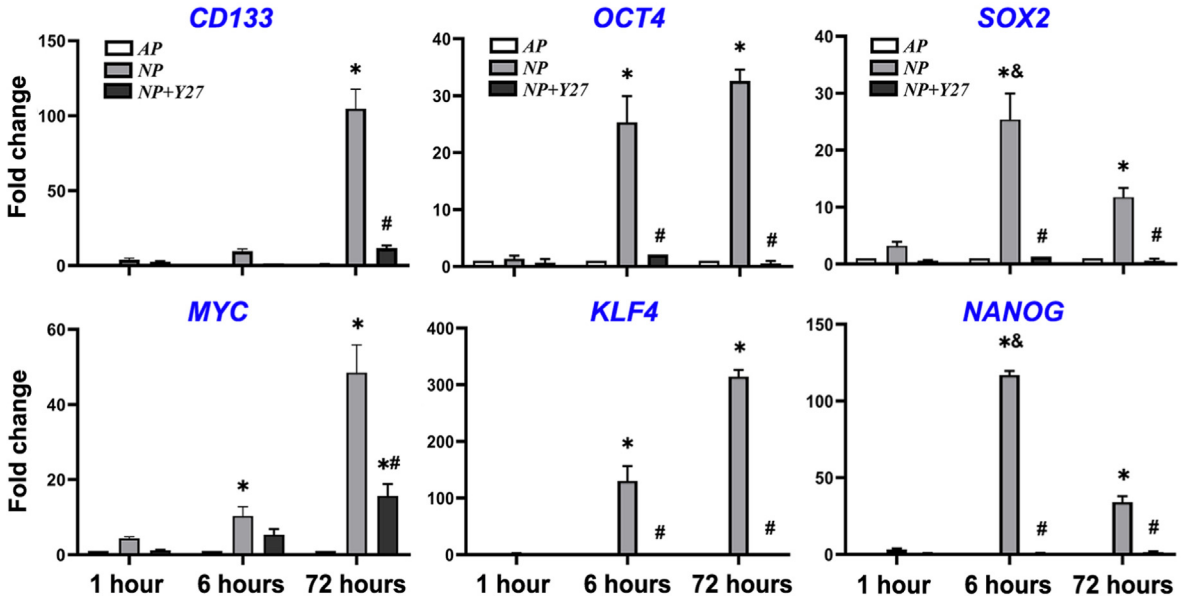

Fig. 3. The expression changes of "stemness" genes in hepatocytes with −50 mmHg stimulation and ROCK inhibitor treatment. qRT-PCR data on the expression of *CD133*, *OCT4*, *SOX2*, *MYC*, *KLF4*, and *NANOG* are shown. All data are presented as mean ± SD from three independent experiments. AP: atmospheric pressure; NP: negative pressure; NP + Y27: negative pressure plus ROCK inhibitor Y27632. $^{*}p < 0.0001$ *vs.* AP group; $^{\#}p < 0.0001$ *vs.* NP group in all time points. $^{\&}p < 0.0001$ NP group at 6 h *vs.* NP group at 72 h.

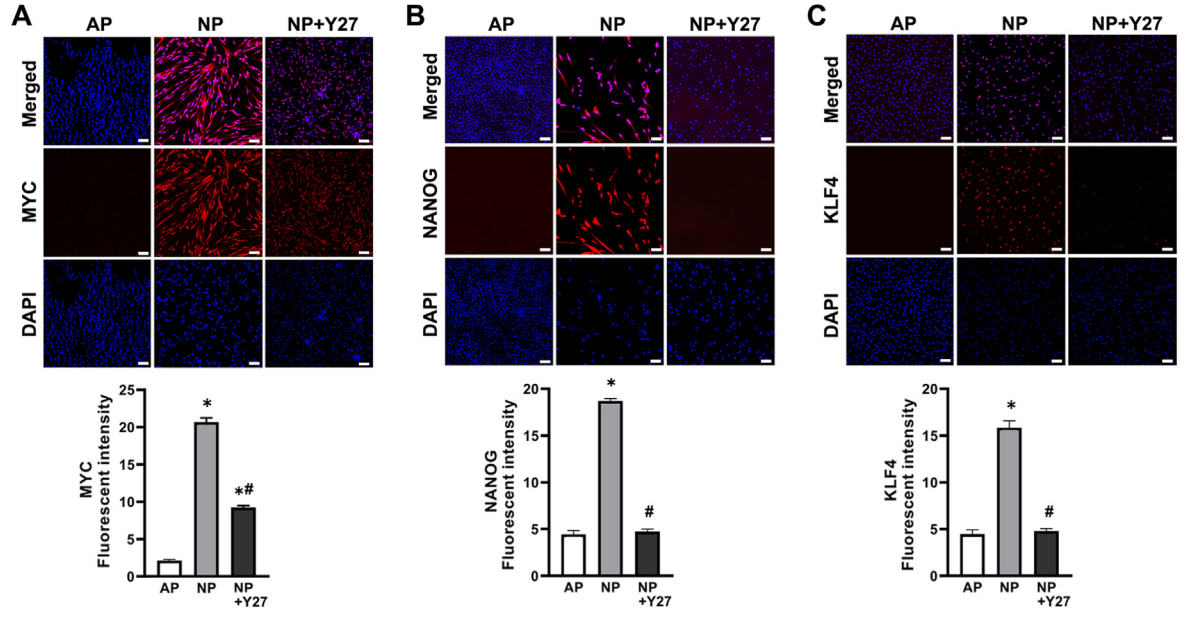

Fig. 4. Immunostaining analysis on the expression of "stemness" marker molecules in hepatocytes at 72 h with −50 mmHg stimulation and ROCK inhibitor treatment. Representative images (upper) and semi-quantitative data (lower) show the protein level of MYC (**A**), NANOG (**B**), and KLF4 (**C**) (scale bars: 100 μm). All data are presented as mean ± SD from three independent experiments. AP: atmospheric pressure; NP: negative pressure; NP + Y27: negative pressure plus ROCK inhibitor Y27632. $^{*}p < 0.05$ *vs* AP group; $^{\#}p < 0.05$ *vs* NP group in all time points.

molecules related to RhoA/ROCK pathway and cell "stemness". However, ROCK inhibitor Y27632 effectively attenuated the almost changes in hepatocytes induced by −50 mmHg stimulation. Based on our experimental data, appropriate negative pressure stimulation may activate the RhoA/ROCK pathway to promote the dedifferentiation of hepatocytes.

Mechanical forces are well known to be critical in cell survival and biological behaviors. It has been demonstrated the benefits of −125 mmHg in improving the healing of an opened wound [18]. A previous study has found that −125 mmHg negative pressure stimulation promotes the differentiation of bone marrow mesenchymal stem cells into osteogenic lineage [19]. Short-time exposure of mesenchymal stem cells to high hydrostatic pressure (−50 KPa≒ −375 mmHg) has been also found to induce osteogenic lineage [20]. In contrast, very high positive pressure (+50 MPa ≒ 37×10^4 mmHg) induces the damage and necrosis of dermal fibroblasts [21]. Thus, the effect of mechanical stresses on cell bioactivity can be largely varied depending on the forces, periods, and patterns of mechanical stresses, as well as the cell types and cell qualities [22]. However, the probable role of negative

pressure on cell dedifferentiation has not yet been investigated. In this study, we found that −50 mmHg is the moderate condition for activating RhoA/ROCK signaling pathway to enhance the expression of marker molecules on "stemness" in hepatocytes.

Cell shape, cytoskeletal tension, and RhoA/ROCK signal have been already determined as the critical factors/regulators on "stem" cell fate [23,24]. ROCK1 and ROCK2, both downstream of RhoA share 65% overall identity and 92% similarity in their kinase domains [25]. ROCKs affect the target downstream of actin polymerization and stress fiber formation, especially under mechanical cues to control the shape and orientation of cells [26,27]. Agreed well with previous report on the quick activation of RhoA/ROCK signal pathway following mechanical stress [28], our data showed that the expression of RhoA and ROCKs was significantly increased within 1 h and continued to 72 h in hepatocytes under −50 mmHg stimulation. As one of the most important mechanotransduction pathways, the activation of RhoA/ROCK signaling transduces the received mechanical stimuli to initiate the transcription of downstream genes, including cytoskeleton-related genes [29,30]. We also observed the formation of F-actin stress fibers, the remarkable change of cell morphology, and the upregulation of FAK (Focal adhesion kinase), SRC (Proto-oncogene tyrosine protein kinase Src), and CDC42 (Cell Division Cycle 42) in hepatocytes under −50 mmHg stimulation.

The actin cytoskeleton polymerization and RhoA/ROCK pathway are well known to regulate cell biological behaviors, including cell differentiation and maturation. Laterally confined growth of fibroblasts on micropatterned substrates induces stem-cell-like spheroid with cytoskeletal gene upregulation and actomyosin contractility [31]. Additionally, it has been demonstrated that mechanical tension affects the actin filaments that arose from substrate stiffness drives human embryonic and canine kidney cells toward a stem-like state [32,33]. RhoA/ROCK pathway has also been demonstrated to play critical roles in the viability and differentiation of stem cells [34,35]. However, it keeps controversial about the role of actin cytoskeleton polymerization and RhoA/ROCKs pathway in cell reprogramming. ROCK inhibitor Y27632 has been demonstrated to improve the post-thaw viability of cryopreserved human embryonic stem cells [36], but conversely promotes the differentiation of endothelial cells from embryonic stem cell-derived Flk1-positive mesodermal precursor cells [37]. A mixture of ROCK inhibitor Y27632 and other small molecule compounds have been used for transferring hepatocytes into proliferative bipotent liver progenitors [38]. On the other hand, either RhoA inhibition or ROCK1/2 knock-down seem to abolish the TGF-β-induced reprogramming process of human corneal endothelial cells [39]. Otherwise, long-time exposure of human-induced pluripotent stem cells to Y-27632 changes cell morphology but shows a very limited effect on the expression of pluripotency markers such as NANOG and OCT4 [40]. However, our data showed a robust enhancement of marker molecules on "stemness" in hepatocytes with −50 mmHg stimulation, suggesting the induction of dedifferentiation. We further demonstrated the dedifferentiation of hepatocytes induced by −50 mmHg stimulation was depended on the activation of RhoA/ROCK signaling pathway. Mechanical cues activate various signaling pathways such as YAP/TAZ, PI3K/AKT, and Wnt/β-catenin, which leads to wide changes on the cellular function and morphology. Therefore, the change of mechanical cues and the dysregulation of mechanotransduction signaling also play a critical role in the development and progression of hepatic cellular carcinoma [41,42].

Although our study provides the first evidence on the cell dedifferentiation effectively induced by −50 mmHg stimulation, we have not yet tried to further evaluate the biological properties of these dedifferentiated hepatocytes. Otherwise, it is highly required to optimize the experimental conditions, including the force of negative pressure and the time of stimulation.

5. Conclusion

In summary, our data revealed that the *ex vivo* exposure of primary human hepatocytes to an appropriate negative pressure (−50 mmHg) activated RhoA/ROCK pathway to effectively induce obvious morphological change and robust upregulation of molecule markers on "stemness", suggesting the induction of cell dedifferentiation. Appropriate mechanical stress stimulation may present a simple and safe method for cell reprogramming.

Funding

This work is a collaborative research program between the Egypt-Japan Education Partnership (EJEP) and the Atomic Bomb Disease Institute of Nagasaki University, and supported by the National Natural Science Foundation of China (81960101). The funder played no role in the study design, data collection, analysis, decision to publish, or preparation of the manuscript.

Contributions

T.L., S.Z., W.Z. concepted and designed the research project. M.O.K. performed the experiments. M.O.K. acquired the data. M.O.K., T.M., K·I., and T.L. analyzed the data. M.O.K. and T.L. wrote the manuscript. All authors discussed the results and approved the manuscript.

Data availability statement

The data that support the findings of this study are available on request from the corresponding author.

Declaration of competing interest

The authors indicate there is no competing of interest.

Acknowledgements

Not applicable.

Appendix A. Supplementary data

Supplementary data to this article can be found online at https://doi.org/10.1016/j.bbrc.2023.05.042.

References

[1] K. Takahashi, K. Tanabe, M. Ohnuki, M. Narita, T. Ichisaka, K. Tomoda, et al., Induction of pluripotent stem cells from adult human fibroblasts by defined factors, Cell 131 (5) (2007) 861–872.
[2] K. Takahashi, S. Yamanaka, Induction of pluripotent stem cells from mouse embryonic and adult fibroblast cultures by defined factors, Cell 126 (4) (2006) 663–676.
[3] G. Liu, B.T. David, M. Trawczynski, R.G. Fessler, Advances in pluripotent stem cells: history, mechanisms, technologies, and applications, Stem Cell Rev Rep 16 (1) (2020) 3–32.
[4] N. Miyoshi, H. Ishii, H. Nagano, N. Haraguchi, D.L. Dewi, Y. Kano, et al., Reprogramming of mouse and human cells to pluripotency using mature microRNAs, Cell Stem Cell 8 (6) (2011) 633–638.
[5] T. Katsuda, J. Matsuzaki, T. Yamaguchi, Y. Yamada, M. Prieto-Vila, K. Hosaka, et al., Generation of human hepatic progenitor cells with regenerative and metabolic capacities from primary hepatocytes, Elife 8 (2019) 1–31.
[6] M. Kiamehr, L. Heiskanen, T. Laufer, A. Düsterloh, M. Kahraman, R. Käkelä, et al., Dedifferentiation of primary hepatocytes is accompanied with reorganization of lipid metabolism indicated by altered molecular lipid and miRNA profiles, Int. J. Mol. Sci. 20 (12) (2019) 2910.

[7] Y. Malato, S. Naqvi, N. Schürmann, R. Ng, B. Wang, J. Zape, et al., Fate tracing of mature hepatocytes in mouse liver homeostasis and regeneration, J. Clin. Invest. 121 (12) (2011) 4850–4860.
[8] D. Mangnall, N.C. Bird, A.W. Majeed, The molecular physiology of liver regeneration following partial hepatectomy, Liver Int. 23 (2) (2003) 124–138.
[9] L.M. Brown, S.R. Rannels, D.E. Rannels, Implications of post-pneumonectomy compensatory lung growth in pulmonary physiology and disease, Respir. Res. 2 (6) (2001) 340–347.
[10] M. Aspal, R.L. Zemans, Mechanisms of ATII-to-ATI cell differentiation during lung regeneration, Int. J. Mol. Sci. 21 (9) (2020) 3188.
[11] R. Fritsch, I. De Krijger, K. Fritsch, R. George, B. Reason, M.S. Kumar, et al., Ras and Rho families of GTPases directly regulate distinct phosphoinositide 3-kinase isoforms, Cell 153 (5) (2013) 1050–1063.
[12] O. Soriano, M. Alcón-Pérez, M. Vicente-Manzanares, E. Castellano, The crossroads between Ras and Rho signaling pathways in cellular transformation, motility and contraction, Genes 12 (6) (2021) 819.
[13] M. Iizuka, K. Kimura, S. Wang, K. Kato, M. Amano, K. Kaibuchi, et al., Distinct distribution and localization of Rho-kinase in mouse epithelial, muscle and neural tissues, Cell Struct. Funct. 37 (2) (2012) 155–175.
[14] H.C. Gao, H. Zhao, W.Q. Zhang, Y.Q. Li, L.Q. Ren, The role of the Rho/Rock signaling pathway in the pathogenesis of acute ischemic myocardial fibrosis in rat models, Exp. Ther. Med. 5 (4) (2013) 1123–1128.
[15] Y. Li, A.S. Mao, B.R. Seo, X. Zhao, S.K. Gupta, M. Chen, et al., Compression-induced dedifferentiation of adipocytes promotes tumor progression, Sci. Adv. 6 (4) (2020) 1–13.
[16] M. Chen, J. Huang, X. Yang, B. Liu, W. Zhang, L. Huang, et al., Serum starvation induced cell cycle synchronization facilitates human somatic cells reprogramming, PLoS One 7 (4) (2012), e28203.
[17] E. Hammar, A. Tomas, D. Bosco, P.A. Halban, Role of the Rho-ROCK (Rho-associated kinase) signaling pathway in the regulation of pancreaticβ-cell function, Endocrinology 150 (5) (2009) 2072–2079.
[18] O. Borgquist, R. Ingemansson, M. Malmsjö, The influence of low and high pressure levels during negative-pressure wound therapy on wound contraction and fluid evacuation, Plast. Reconstr. Surg. 127 (2) (2011) 551–559.
[19] J. Zhu, A. Yu, B. Qi, Z. Li, X. Hu, Effects of negative pressure wound therapy on mesenchymal stem cells proliferation and osteogenic differentiation in a fibrin matrix, PLoS One 9 (9) (2014), e107339.
[20] Y.G. Zhang, Z. Yang, H. Zhang, C. Wang, M. Liu, X. Guo, et al., Effect of negative pressure on human bone marrow mesenchymal stem cells in vitro, Connect. Tissue Res. 51 (1) (2010) 14–21.
[21] T.M. Le, N. Morimoto, N.T.M. Ly, T. Mitsui, S.C. Notodihardjo, M.C. Munisso, et al., Hydrostatic pressure can induce apoptosis of the skin, Sci. Rep. 10 (1) (2020), 17594.
[22] E. Tworkoski, M.R. Glucksberg, M. Johnson, The effect of the rate of hydrostatic pressure depressurization on cells in culture, PLoS One 13 (1) (2018) 1–21.
[23] M.D. Treiser, E.H. Yang, S. Gordonov, D.M. Cohen, I.P. Androulakis, J. Kohn, et al., Cytoskeleton-based forecasting of stem cell lineage fates, Proc. Natl. Acad. Sci. U.S.A. 107 (2) (2010) 610–615.
[24] R. McBeath, D.M. Pirone, C.M. Nelson, K. Bhadriraju, C.S. Chen, Cell shape, cytoskeletal tension, and RhoA regulate stem cell lineage commitment, Dev. Cell 6 (4) (2004) 483–495.
[25] O. Nakagawa, K. Fujisawa, T. Ishizaki, Y. Saito, K. Nakao, S. Narumiya, ROCK-I and ROCK-II, two isoforms of Rho-associated coiled-coil forming protein serine/threonine kinase in mice, FEBS Lett. 392 (2) (1996) 189–193.
[26] A. Roshanzadeh, T.T. Nguyen, K.D. Nguyen, D.S. Kim, B.K. Lee, D.W. Lee, et al., Mechanoadaptive organization of stress fiber subtypes in epithelial cells under cyclic stretches and stretch release, Sci. Rep. 10 (1) (2020), 18684.
[27] A.M. Greiner, H. Chen, J.P. Spatz, R. Kemkemer, Cyclic tensile strain controls cell shape and directs actin stress fiber formation and focal adhesion alignment in spreading cells, PLoS One 8 (10) (2013), e77328.
[28] S.T. Boyle, J. Kular, M. Nobis, A. Ruszkiewicz, P. Timpson, M.S. Samuel, Acute compressive stress activates RHO/ROCK-mediated cellular processes, Small GTPases 11 (5) (2020) 354–370.
[29] A.S. Torsoni, T.M. Marin, L.A. Velloso, K.G. Franchini, RhoA/ROCK signaling is critical to FAK activation by cyclic stretch in cardiac myocytes, Am. J. Physiol. Heart Circ. Physiol. 289 (4) (2005) H1488–H1496.
[30] B. Xu, G. Song, Y. Ju, X. Li, Y. Song, S. Watanabe, RhoA/ROCK, cytoskeletal dynamics, and focal adhesion kinase are required for mechanical stretch-induced tenogenic differentiation of human mesenchymal stem cells, J. Cell. Physiol. 227 (6) (2012) 2722–2729.
[31] B. Roy, L. Yuan, Y. Lee, A. Bharti, A. Mitra, G.V. Shivashankar, Fibroblast rejuvenation by mechanical reprogramming and redifferentiation, Proc. Natl. Acad. Sci. U.S.A. 117 (19) (2020) 10131–10141.
[32] M.E. Melica, G. La Regina, M. Parri, A.J. Peired, P. Romagnani, L. Lasagni, Substrate stiffness modulates renal progenitor cell properties via a ROCK-mediated mechanotransduction mechanism, Cells 8 (12) (2019) 1561.
[33] J. Guo, Y. Wang, F. Sachs, F. Meng, Actin stress in cell reprogramming, Proc. Natl. Acad. Sci. U.S.A. 111 (49) (2014) E5252–E5261.
[34] L. Hyväri, M. Ojansivu, M. Juntunen, K. Kartasalo, S. Miettinen, S. Vanhatupa, Focal adhesion kinase and ROCK signaling are switch-like regulators of human adipose stem cell differentiation towards osteogenic and adipogenic lineages, Stem Cell. Int. 2018 (2018), 2190657.
[35] P. Mistriotis, V.K. Bajpai, X. Wang, N. Rong, A. Shahini, M. Asmani, et al., Nanog reverses the myogenic differentiation potential of senescent stem cells by restoring actin filamentous organization and SRF-dependent gene expression, Stem Cell. 35 (1) (2017) 207–221.
[36] B.C. Heng, Effect of Rho-associated kinase (ROCK) inhibitor Y-27632 on the post-thaw viability of cryopreserved human bone marrow-derived mesenchymal stem cells, Tissue Cell 41 (5) (2009) 376–380.
[37] H.J. Joo, D.K. Choi, J.S. Lim, J.S. Park, S.H. Lee, S. Song, et al., ROCK suppression promotes differentiation and expansion of endothelial cells from embryonic stem cell-derived Flk1+ mesodermal precursor cells, Blood 120 (13) (2012) 2733–2744.
[38] T. Katsuda, M. Kawamata, K. Hagiwara, R.u. Takahashi, Y. Yamamoto, F.D. Camargo, et al., Conversion of terminally committed hepatocytes to culturable bipotent progenitor cells with regenerative capacity, Cell Stem Cell 20 (1) (2017) 41–55.
[39] Y.-T. Zhu, F. Li, B. Han, S. Tighe, S. Zhang, S.-Y. Chen, et al., Activation of RhoA-ROCK-BMP signaling reprograms adult human corneal endothelial cells, J. Cell Biol. 206 (6) (2014) 799–811.
[40] S.I. Vernardis, K. Terzoudis, N. Panoskaltsis, A. Mantalaris, Human embryonic and induced pluripotent stem cells maintain phenotype but alter their metabolism after exposure to ROCK inhibitor, Sci. Rep. 7 (2017), 42138.
[41] D. Esposito, I. Pant, Y. Shen, R.F. Qiao, X. Yang, Y. Bai, et al., ROCK1 mechano-signaling dependency of human malignancies driven by TEAD/YAP activation, Nat. Commun. 13 (1) (2022) 703.
[42] D. Gnani, I. Romito, S. Artuso, M. Chierici, C. De Stefanis, N. Panera, et al., Focal adhesion kinase depletion reduces human hepatocellular carcinoma growth by repressing enhancer of zeste homolog 2, Cell Death Differ. 24 (5) (2017) 889–902.

Supplementary Table 1: Primary antibodies used for experiments.

Antibodies	Host Animal	Catalog No.	Dilution	Manufacturer
ROCK1	pRabbit	ab156284	1/250	Abcam
ROCK2	pRabbit	ab71598	1/250	
CK19	mRabbit	ab52625	1/200	
KLF4	mRabbit	#4038	1/400	Cell Signaling
NANOG	mRabbit	D73G4	1/800	
C-Myc	mRabbit	D84C12	1/800	

p: polyclonal antibody & m: monoclonal antibody

Supplementary Table 2: Secondary antibodies used for experiments.

Antibodies	Host Animal	Catalog No.	Dilution	Manufacturer
Alexa Flour (Plus 488)	Rabbit	#A32731	1/500	Invitrogen
Alexa Flour (546) IgG (H+L)	Rabbit	#A-11035	1/500	Invitrogen

Supplementary Table 3: Primers used for qRT-PCR experiments.

Human Target Genes	5'-Forward Primer-3'	5'-Reverse Primer-3'
CD133	GCCCCCAGGAAATTTGAGAAC	GCTTTGGTATAGAGTGCTCAGTG
CDC42	GCCCGTGACCTGAAGGCTGTCA	TGCTTTTAGTATGATGCCGACACCA
FAK	GAAGCATTGGGTCGGGAACTA	CTCAATGCAGTTTGGAGGTGC
GAPDH	CCCCGGTTTCTATAAATTGAG	CACCTTCCCCATGGTGTCT
KLF4	GTCCGACCTGGAAAATGCTC	TGGCAGTGTGGGTCATATCC
MYC	CCTGGTGCTCCATGAGGAGAC	CAGACTCTGACCTTTTGCCAGG
NANOG	TCCTGCAGTGCCCGAAAC	GGTCTGGTTGCTCCACATTG
OCT4	TCCTGCAGTGCCCGAAAC	TCAAAATCCTCTCGTTGTGCATA
RHOA	CAGAAAAGTGGACCCCAGAA	GCATGCTGCTCTCGTAGCCATTTC
ROCK1	AACATGCTGGATAAATCTGG	TGTATCACATCGTACCATGCC
ROCK2	TCAGAGGT CTACAGATGAAGGC	CCAGGGGCTATTGGCAAAGG
SOX2	ACAGCATGATGCAGGACCAG	CTGCTGCGAGTAGGACATGC
SRC	CAGTGTCTGACTTCGACAACGC	CCATCGGCGTGTTTGGAGTA